- IDEALFUEL -

Lignin as a feedstock for renewable marine fuels

GRANT AGREEMENT No. 883753

HORIZON 2020 PROGRAMME - TOPIC LC-SC3-RES-23-2019
"Development of next generation biofuel and alternative renewable fuel technologies for aviation and shipping"

Deliverable Report

D5.3 – 4-Stoke research engine - Validation of the CFD models with experiments

This project has received funding from the European Union's Horizon 2020 research and innovation programme under grant agreement No 883753

Deliverable No.	IDEALFUEL D5.3	
Related WP	WP5	
Deliverable Title	Modeling 2- and 4- stroke engine	
Deliverable Date	27-03-2024	
Deliverable Type	REPORT	
Dissemination level	Confidential – consortium members only (CO) / Classified (CL) / Public (PU)	Public (PU)
Written By	Andrea Di Matteo (TU/e)	27-03-2024
Checked by	Bart Somers (TU/e)	28-04-2023
Reviewed by	WINGD	29-04-2024
Approved by	Roy Hermanns (TUE)	29-04-2024
Status	FINAL	30-04-2024

Disclaimer/ Acknowledgment

This project has received funding from the European Union's Horizon 2020 research and innovation programme under grant agreement No 883753. The information and views set out in this publication does not necessarily reflect the official opinion of the European Commission. Neither the European Union institutions and bodies nor any person acting on their behalf, may be held responsible for the use which may be made of the information contained therein.

Publishable summary

This report addresses the need for the numerical modelling of the combustion chamber where the new Bio-HFO will be tested. Computational Fluid Dynamics (CFD) is a powerful tool that allows to reproduce the physics of fluids and improve consequently the design of the volume of interest. To do that, the latter is subdivided in multiple smaller volumes, to create a so-called mesh. Here the mathematical equations describing the fluids behavior, the Navier-Stokes, are solved. However, provided the limited computational resources the simulations can rely on, mathematical models are requested to simplify the approach, i.e. turbulence modelling, and to implement additional modules, i.e. combustion modelling.

Main goal of this deliverable is to create and validate with experiments a reliable and computationally efficient computational set-up for the so-called Spray Combustion Chamber (SCC), a constant volume chamber created by the project partner WinGD to study spray injection and non-premixed combustion. Therefore, first the analysis has focused on the validation of the ensemble of models on simplified, smaller and well-known cases, namely the ECN Diesel Sprays A, C and D. Then, provided the reliability of the outcome, the same models have been used to simulate the SCC in single- and multi-nozzle configuration, where the results have shown good agreement with the experimental data provided by the company.

The work led to the following steps and thus conclusions, which reflect the logic path described above:

- The performance of a computationally expensive (LES) and less-expensive (RANS) turbulence model have been assessed and compared for two ECN Sprays, C and D, using a tabulated combustion model, namely Flamelet Generated Manifold (FGM). The latter decouples the computational effort requested by the chemical calculations for the combustion development from the one related to the fluid behavior. This leads to the convenient possibility of using a detailed mechanism for the fuel, without worrying much about its negative impact on the computational performance.
  The main conclusion of this work is that the efficient RANS turbulence model coupled with the FGM combustion model provide comparable results to the more detailed LES.
- Given the large difference in size between the nozzles used as benchmark and the ones in the SCC, a study on the influence of the nozzle diameter on the combustion properties has been carried out. It was found that the Ignition Delay Time and Lift-Off Length follow a quadratic dependency with respect to the nozzle diameter, while the Ignition Location is hardly dependent on it.
- Eventually, the same settings and model have been used for the SCC in single- and multi-nozzle configuration. For the first, another similar effort was present in literature, while for the second this was a first time. Therefore, a careful comparison of the numerical outcome with the experimental data, led to promising results in terms of the main combustion parameters.

In conclusion, the combination of the RANS turbulence model and the FGM combustion model has proven to be very efficient and reliable in the analysis of such injectors and volume sizes and embodies a solid base to test the future Bio-Fuel.

Contents

Table of Figures

Tables

Abbreviations

Symbol / short name	
ECN	Engine Combustion Network
SCC	Spray Combustion Chamber
RANS	Reynolds-Averaged Navier-Stokes
LES	Large Eddy Simulations
FGM	Flamelet Generated Manifold
LTC	Low Temperature Combustion
HTC	High Temperature Combustion
IDT	Ignition Delay Time
LOL	Lift-Off Length
IL	Ignition Location
HRR	Heat Release Rate
Pave	Average Pressure in Chamber

1 Introduction

To successfully address the performance of the bio-HFO and assess the operational limits without vey elaborate and expensive test procedures and/or prototyping often CFD modelling is employed. Since a key element of the project will be dependence of the performance on the composition of the bio-HFO, detailed chemical models that describe the combustion are necessary. Given the size of the engine and the complexity and shear size of the chemical models, an efficient 'combustion-model' needs to be used. The Flamelet Generated Manifold method is such an method and has been validated for benchmark experiments and smaller engines. This report addresses the development of this approach for two- and four-stroke marine engines. The envisaged route, as is reflected in the set-up of Workpackage 5, was a thorough validation of the approach on the unique constant volume chamber (termed SCC, see D5.4) first for a reference fuel and then the bio-HFO. After that validation the model would be applied to a small four-stroke engine (because it needs only a few 10-100 liters of bio-HFO) after which, it would be applied to a full-size two-stroke marine engine. However, the failure to produce the bio-HFO on a larger scale, made that the campaigns on the engines were not performed. Hence, this deliverable solely focusses on the development of the method and a through validation on the experiments of the constant volume set-up for the reference fuel. This is a significant step and the first attempt ever as far as we know using FGM for such big engines.

Computational Fluid Dynamics (CFD) is a powerful tool that allows us to study systems which involve (turbulent) flows and combustion in complex time-varying geometries. To do that, the latter are subdivided in multiple smaller volumes, to create a so-called mesh. Here the mathematical equations describing the fluids behavior, the Navier-Stokes, are discretized. However, given the large number of degrees of freedom and limited computational resources certain details need to be modelled, e.g. turbulence, combustion, and wall effects.
Main aspect of this deliverable is a reliable and computationally efficient computational set-up for the so-called Spray Combustion Chamber (SCC), a constant volume chamber in use at the project partner WinGD to study spray injection and non-premixed combustion at conditions as they occur in large two-stroke engines. Therefore, first the analysis is focused on the validation of the ensemble of sub-models on simplified, smaller, and well known and well documented cases, namely the ECN Diesel Sprays A, C and D. Then, the same models have been used to simulate the SCC in single- and multi-nozzle configuration.

Spray diesel combustion in constant volume chambers is extensively investigated in literature. Experimental studies have helped in the description of the non-premixed combustion process [1; 2] as a multi-stage process: a first stage lean ignition occurs, leading to a low temperature combustion (LTC) whose onset is mainly governed by chemical kinetics; a turbulent cool flame wave spreads the LTC products and provides quasi-homogeneous mixture, where a second stage rich ignition occurs, leading to a high temperature combustion (HTC); a turbulent flame propagates, stabilizing afterwards at a distance from the nozzle where both diffusion flames and premixed reaction zones coexist. These stages have been well studied and reproduced in highly resolved numerical efforts [3]. A pivotal role in the understanding of diesel combustion, is played by the Engine Combustion Network (ECN)[4], which provide a database of experimental data on standard injectors, ranging from passenger-like nozzles (Spray A) to heavy-duty-like nozzles (Spray C and D). Based on ECN spray benchmarks, both experimental [5] and numerical [6] works are available. The authors show in [7] a numerical comparison between Spray C and D in the framework of RANS and LES turbulence modelling. The results for the first proved to be consistent with the experiments and with a more accurate model as the second. Therefore, the approach is deemed reliable for the following steps of this study, i.e. its application on the large constant volume chamber SCC.

The SCC has already been studied, both experimentally and numerically. In [8; 9] a first base dataset of the inert spray is presented. In [4], both single- and multi-nozzle configurations are analyzed, focusing on the relevance of a co- or counter-swirl injection in the resulting spray penetration. The second work focuses more on the single-nozzle configuration to study the role of swirl, density, and evaporation. In [10] a post-processing technique, based on shadow imaging, is proposed to locate a spray contour and angle. Reacting conditions of the single-nozzle configuration are analyzed in [11] in terms of ignition delay time (IDT), lift-off length (LOL) and ignition location (IL) at different temperatures inside the domain. Here the strong interaction between the flame and the liquid spray (the ignition spot is found to be at about half of the liquid length) is observed. This differs from smaller heavy-duty nozzles where this interaction is much less. First CFD studies are presented in [12], where a grid sensitivity study on the single-nozzle configuration showed the best results with a minimum mesh size of

approximately twice the injector diameter. However, a similar study by the authors published in [13] showed better agreement for smaller size, up to ½ of the nozzle diameter. In [14] a study on the influence of the nozzle size on the ignition behavior is shown. A similar study by the authors [13] has retrieved mathematical relationships between the main combustion parameters of large naval-size nozzles and the benchmark Spray D.
These studies gave a huge insight into the understanding of diesel combustion, ECN sprays and large marine size injectors having a simple layout (a single hole). Therefore, the approach for realistic multi-nozzle injectors is deemed solid. In the next section (2) the approach will be introduced shortly. In 3, the results for the single hole nozzles will be presented as well as the final model for the multi-hole nozzle. Finally, a conclusion will be formulated in 4.

2 Methods

2.1 Software

The widely used open-source CFD software OpenFOAM [15] is used for this work. The numerical schemes are a mix of first/second order discretization schemes. All the simulations were run in a single node of the cluster at the TU/e, confirming the moderate computational demands. For a wide variety of applications, it is difficult to attain accurate CFD simulation results without approximating the turbulence and combustion with models. Resolving all time and length scales is simply impossible. In 2.2 the turbulence modelling and in 2.3 the combustion modelling is introduced.

2.2 Turbulence Modelling

Turbulence significantly increases the rate of mixing of momentum, energy, and species. It is common to use models to mimic the additional mixing coming from the turbulence scales which are not resolved. Two main approaches exist, RANS (2.2.1) and LES (2.2.2) which are shortly described in the two upcoming sections.

2.2.1 RANS

For the Reynolds-Averaged Navier-Stokes (RANS), the fields are decomposed into a mean value and a fluctuating term. This decomposition is substituted in the Navier-Stokes equations, introducing, however, the so-called Reynolds stresses τ_{ij}, for which closures must be introduced. One of the most widely used is the $k-\varepsilon$ model, where two additional transport equations, one for the turbulent kinetic energy k and one for the dissipation of the turbulent kinetic energy ε, are introduced to build the turbulent viscosity μ_t:

$$\mu_t = C_\mu \rho \frac{k^2}{\varepsilon}$$

that is used to compute τ_{ij}.
This model is widely used in many applications since it is affordable in terms of computational cost and reliable in terms of results. The drawback is mainly in the level of detail that can be achieved, since the method averages the values of the domain, making the local variations less accurate.

2.2.2 LES

For the Large Eddy Simulation (LES) approach, the fields are decomposed in a resolved field and a sub-grid field. The first is defined as a spatial average, not as an ensemble average as in RANS. The decomposition is substituted in the Navier-Stokes equations, and like for RANS, Reynolds stresses τ_{ij} appear. These must be formulated in a closed form as well. The most famous approach is the Smagorinsky zero-equation model, where the stress is defined as

$$\tau_{ij} = \bar{\rho} C_s \Delta^2 \left| \sqrt{2 \tilde{S}_{ij} \tilde{S}_{ij}} \right|$$

However, this relation introduces the constant C_s which is case dependent. To mitigate this case-dependency, in this work, a one-equation model is used. Here the stress is defined as

$$\tau_{ij} = 2 k c_{ij}$$

where k is the turbulent kinetic energy for which an additional transport equation is solved, while c_{ij} is a tensor defining the constant dynamically depending on local conditions. Consequently, the model is more flexible.
The LES approach is reliable and provides detailed results, also on local values. However, its computational cost is higher compared to RANS's, since its accuracy is directly linked to the sub-grid filter dimension, i.e. the cell size. The smaller the cell size, the higher the resolved part of the variables, the more accurate the approach, the more expensive the simulation. In many applications, and especially for the large domains of the target application in this part of the project, i.e. marine size two-stroke engines, LES is unfeasible.

2.3 Combustion Modelling

2.3.1 Flamelet Generated Manifold

The Flamelet Generated Manifold (FGM) method [16] is a tabulated chemistry reduction approach that retrieves the thermophysical properties from a pre-computed flamelet database as function of the so-called control

variables (CV). When simulating combustion for each species (N in total) present in the chemical reaction models a conservation equation needs to be solved on top of the conservation equations for momentum and energy (4). N can range from 50-3000 for practical fuels. The idea is to split the computational effort needed to simulate the combustion process from the one implied by the flow solution. This is achieved by the flamelet concept, as formulated in [17], that allows to describe the actual flame as an ensemble of multiple one-dimensional canonical flames. For Diesel-like sprays, a counterflow flame setup as in Fig.1 is the relevant canonical configuration. These one-dimensional flames are used to define the structure on a local scale.

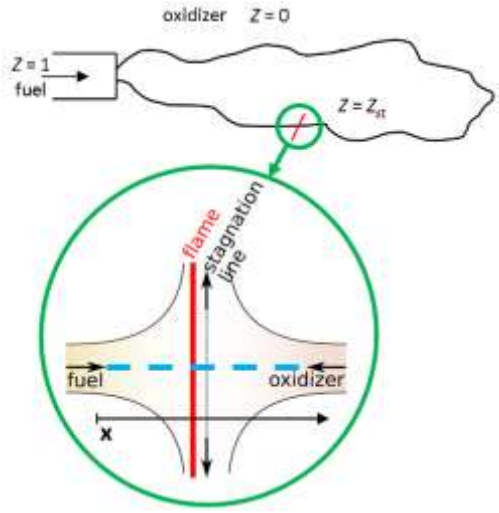

Figure 1: The counter-flow flame concept

The flames are solved along the symmetry axis (blue dashed line) as function of space (x) and time (t). At this point, all the species and the thermodynamic variables are stored. To use this information tables (manifolds), are created using a coordinate transformation. Control variables (CV) are introduced. These are chosen beforehand and in this work are mixture fraction (Z) and combustion progress (Yc) enthalpy (h). To account for turbulence-chemistry interaction a presumed probability density function approach (e.g. beta-pdf, [17]) is implemented. This is also tabulated by pre-computing the pdf-integration using relevant values of the variance of the mixture fraction Zvar. In the CFD model only the transport equations for the controlling variables are solved, instead of one for each species, and based on their values all the species and thermodynamic variables are retrieved from the tables. This method allows the application of detailed chemical mechanisms with acceptable computational costs. To study the effects of the fuel composition on the performance in the two-stroke engines, the application of detailed mechanisms is a pre-requisite. The FGM model allows that at strongly reduced computational costs.

2.4 Liquid modelling

The spray injection is a crucial aspect of the modeling process. The high-pressure liquid spray from the injector nozzle is made of billions of droplets which break-up into smaller ones under the stress of the drag forces and the instabilities of the surface, following a mechanism often referred to as Primary and Secondary Break-up. However, it is computationally impossible to follow every single droplet, given their large number. Therefore, clusters of droplets with the same characteristics, called parcels, are introduced, and followed in the domain instead. To mimic the break-up process, several models are available, mostly differing in the type of forces acting on the parcels and in the separation between the two phases of the process. In this work, the widely used Kelvin-Helmholtz and Rayleigh-Taylor (KH-RT, [24]) model for these types of sprays, is applied in all the simulations.

2.4.1 KH-RT Break-up Model

The KH part of the model is considered for the primary breakup phase. It assumes that the droplet with radius r breaks up due to a surface instability wave into smaller droplets of radius r_c, defined by

$$r_c = B_0 \Lambda_{KH}$$

where Λ_{KH} is the wavelength with maximum grow rate and B_0 is a model constant. The smaller B_0, the smaller the droplet size after break-up. The rate of development of the parent droplet is calculated as

$$\frac{dr}{dt} = \frac{r - r_c}{\tau_{KH}}$$

where τ_{KH} represents the break-up time:

$$\tau_{KH} = \frac{3.726 B_1 r}{\Lambda_{KH} \Omega_{KH}}$$

with Ω_{KH} the maximum grow rate of the wavelength Λ_{KH} and B_1 another model constant.

The RT part of the model is activated for the secondary breakup. It predicts the instabilities on the droplet surface. If the wavelength is smaller than the droplet diameter, RT instabilities are supposed to be growing on the droplet surface. This growth time is compared to the breakup time,

$$\tau_{RT} = \frac{C_\tau r}{\Omega_{RT}}$$

where C_τ is a constant of the model and Ω_{RT} is the wave number of the fastest growing instability wave.

3 Results

3.1 Engine Combustion Network reference cases

In this section, the results are shown according to the following path: first the well-known ECN sprays C and D are analyzed with FGM as combustion model, using both RANS and LES; secondly the RANS+FGM set of models is employed to study the dependence of the main combustion parameters over the nozzle diameter size. Nozzle size is the principal difference between heavy-duty and marine size engines; finally, a complete set-up for the SCC is prepared and validated against experiments. The SCC introduces relevant new complexities compared to the ECN sprays, a swirling gas motion and multi-nozzle injectors. This is investigated systematically.

3.1.1 ECN Sprays

Spray C and D are heavy-duty like injectors that are studied using a simple cylindrical domain, with a structured mesh and a refinement close to the nozzle exit, as pictured in Fig.2. The minimum cell-size and the meshes have been validated with non-reacting simulations comparing liquid length and spray penetration to the experimental values. Note that the minimum cell size is different for the two turbulence models used. In fact, the LES approach requires a smaller cell size (125µm versus 225µm) leading to 2.8Mio cells for LES and 0.75Mio for the RANS respectively.

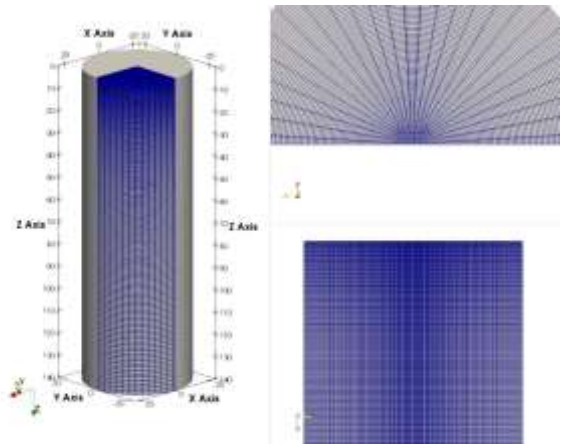

Figure 2: Spray C and D domain and mesh

Temperature [K]	900
Pressure [bar]	60
Swirl [-]	No
N2 [-]	0.75
O2 [-]	0.15
CO2 [-]	0.062
H2O [-]	0.036

Table 1: Initial condition ECN Spray C/D

Once the mesh has proven to be adequate, it is employed to run reacting simulations, for both sprays in RANS and LES frameworks. In Table 1 the initial condition used in the domain are shown.

The results are compared in terms of IDT and LOL, that are defined using a recommended threshold (2% of the maximum, ECN guidelines) for a high temperature combustion product, mostly OH. In Fig.3 and 4, the so-called I_{xt}-plots [5] for Spray C and D are depicted. These show the radially integrated intensity of OH along the axial distance from the nozzle exit in time are often used to extract relevant data and. The colors from blue to red indicate the intensity of OH from low to high. The IDT time (magenta circle) and LOL (white line) are indicated in the figures.

(a) (b)

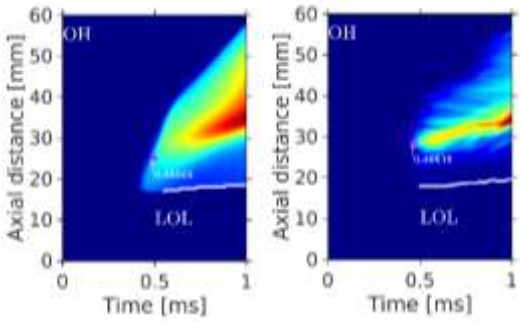

Figure 3: I_{xt}-plots for Spray C RANS (a) and LES (b)

SC	RANS	LES	EXP
IDT [ms]	0.49	0.47	0.56
LOL [mm]	19	20	23.6

Table 2: Results Spray C

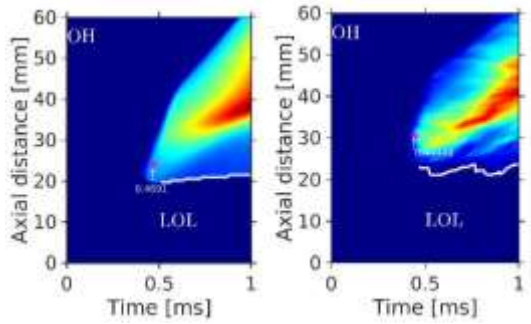

Figure 4: I_{xt}-plots for Spray D RANS (a) and LES (b)

SD	RANS	LES	EXP
IDT [ms]	0.47	0.44	0.56
LOL [mm]	21	23.5	25

Table 3: Results Spray D

Due to the nature of the approach the LES results show larger fluctuations of the intensities which can be reduced by performing more 'realizations'. Earlier studies have shown that for the parameters IDT and LOL, one realization is adequate [23]. Numerical results for both models are similar and in line with experimental values. Both sprays show shorter IDTs than experimental values with the two turbulence models: this can be attributed to the Yao et al. [18] mechanism, as was already found in literature [19]. Note that for both sprays the LOL predicted in RANS is shorter than that in LES, while the IDT is longer than that in LES. It is important to underline that both approaches reproduce the experimental trend well: Spray C has a shorter LOL, Spray D a shorter IDT. In Fig. 5 a temporal flame evolution of Spray C (a) and D (b) is pictured.

The most important species for the combustion analysis are shown in the central rows (white background) of each line: OH, CH_2O and C_2H_2. The first and the second are respectively indicators of high and low temperature combustion, the third is considered a precursor of soot production. Moreover, for each line, in the first and third rows are shown, spatial distributions of mixture fraction, variance of mixture fraction and temperature. In all the rows, LES is the top and RANS simulation is given in the bottom. In both sprays, it can be noted that CH_2O appears mainly in the rich side, close to the droplets, while OH appears afterwards around the stoichiometric mixture fraction, in the zone of high temperatures. This is expected and confirmed in literature [3]. Besides, the high temperature combustion appears on the periphery of the spray plumes, as opposed to smaller passenger-car injectors like Spray A where it occurs at the spray tip [6]. The distribution of C_2H_2, which is a product of rich combustion, appears within the flame core, not far from the stoichiometric mixture fraction and from the high-temperature zone for both simulations. In RANS it initializes earlier than in LES. Afterwards, the maximum intensity of C_2H_2 for both models is identical and moves towards the spray tip, which becomes more and more rich and hot.

To sum up, the local characteristics as well as the main combustion performance indicators are similar in LES and RANS. Therefore, RANS remains a good choice in terms of efficiency, since the computational effort requested is lower and the reproduction of the main parameters is close to the LES. These results are analyzed in more detail in a paper by the authors of this report [7].

Spray C

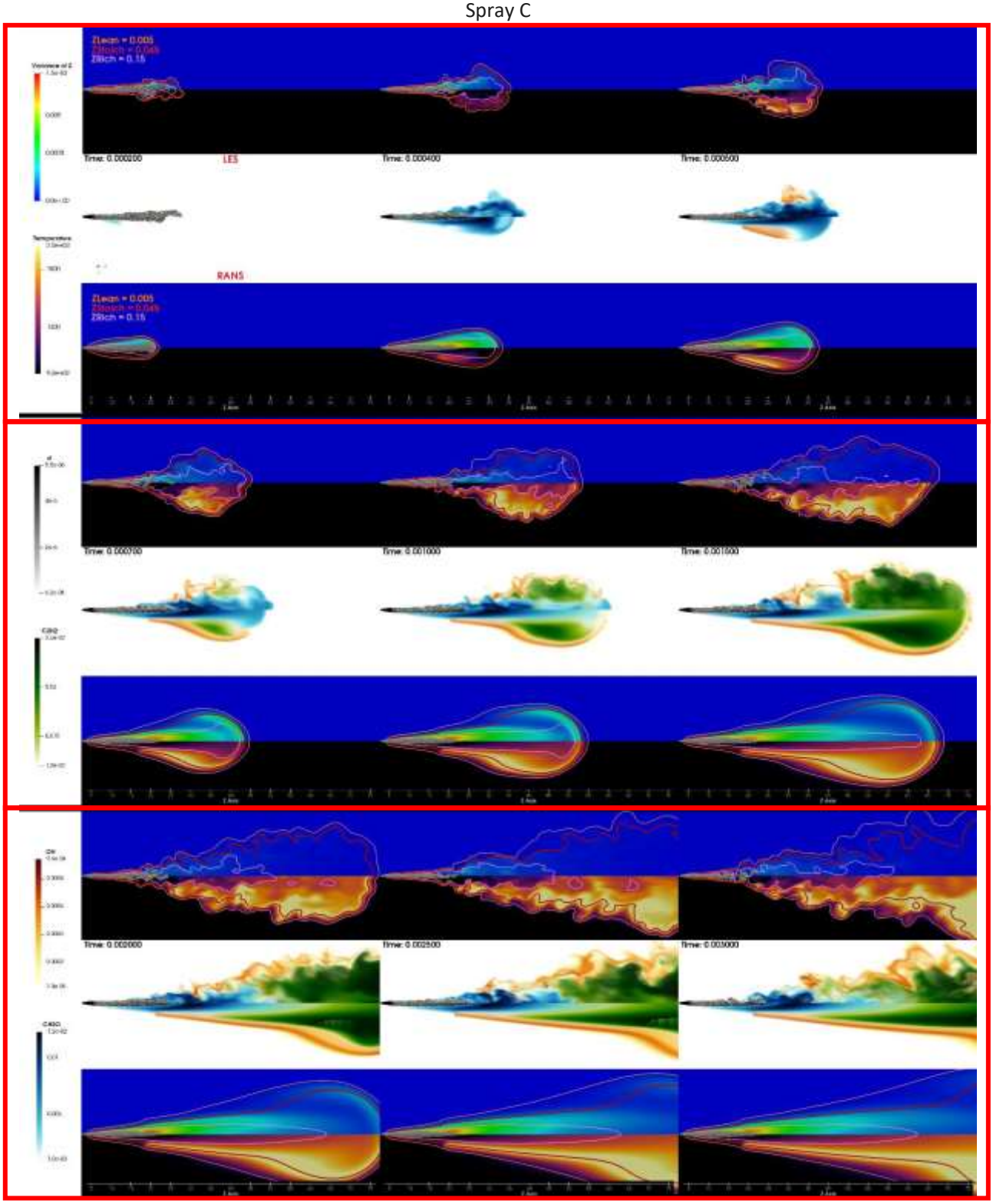

Figure 5a: Spray C flame evolution from 0.2ms to 3ms. The image is divided in three parts: first from 0.2 to 0.5ms, second from 0.7 to 1.5ms and last from 2 to 3ms. Each part is divided in three: the central image (white background) represents OH, CH2O and C2H2 for LES (up) and RANS (down). The surrounding images are temperature distribution, variance of mixture fraction and three contours of Mixture fraction (lean, stoichiometric, and rich) for the LES (top, blue background) and RANS (bottom, blue background).

Spray D

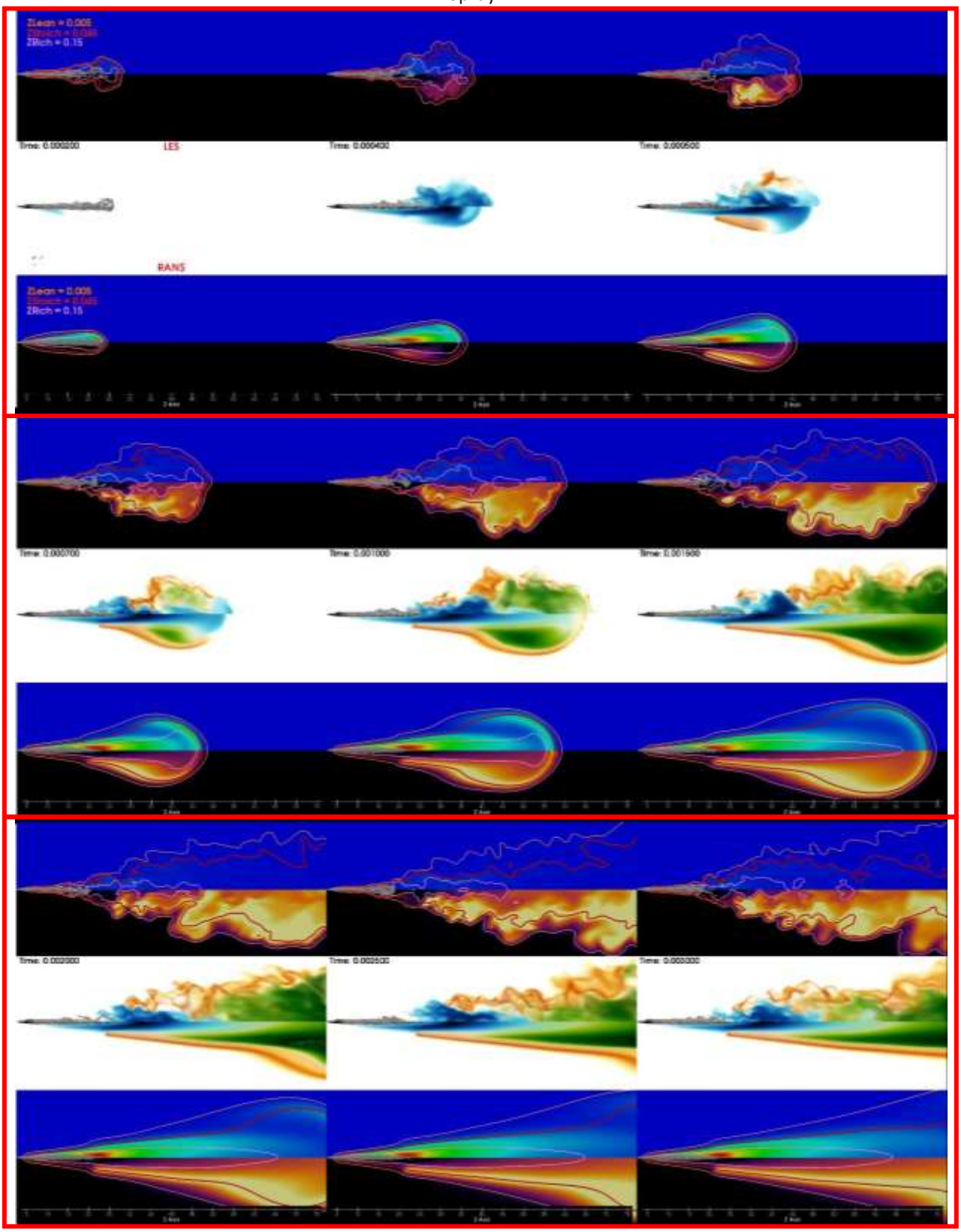

Figure 5b: Spray D flame evolution from 0.2ms to 3ms. The image is divided in three parts: first from 0.2 to 0.5ms, second from 0.7 to 1.5ms and last from 2 to 3ms. Each part is divided in three: the central image (white background) represents OH, CH2O and C2H2 for LES (up) and RANS (down). The surrounding images are temperature distribution, variance of mixture fraction and three contours of Mixture fraction (lean, stoichiometric, and rich) for the LES (top, blue background) and RANS (bottom, blue background).

3.1.2 The influence of the nozzle diameter

A further step in the project is to test the accuracy of the model configuration RANS+FGM used for the ECN sprays on larger nozzles, as they occur in marine applications. Therefore, first a mesh for the SCC is created and validated in inert conditions, with n-dodecane injected with a single nozzle injector of 875µm diameter size (here after referred to as **Test Case**). Then, the same mesh has been used injecting with other **nozzle sizes** (300, 600, 725, 825µm) in reacting conditions and the combustion parameters (IDT, LOL, IL) have been determined and compared to the same for the Spray D benchmark.

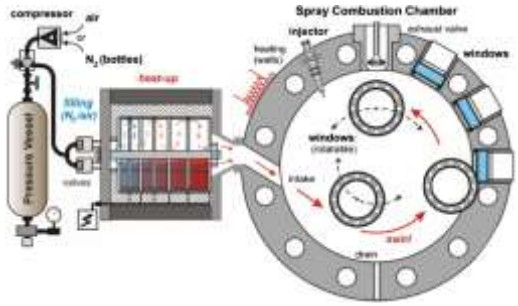

Figure 6: Scheme of the real facility.

Temperature [K]	900
Pressure [bar]	90
Swirl [-]	Yes
N2 [-]	0.767
O2 [-]	0.233
CO2 [-]	0.0
H2O [-]	0.0

Table 4: Initial condition Single-Nozzle configuration

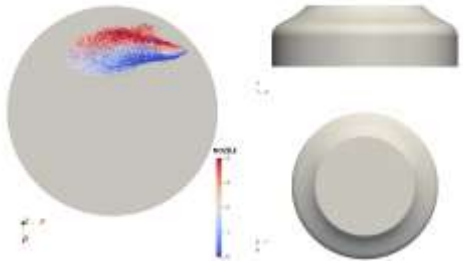

Figure 7: CFD Domain.

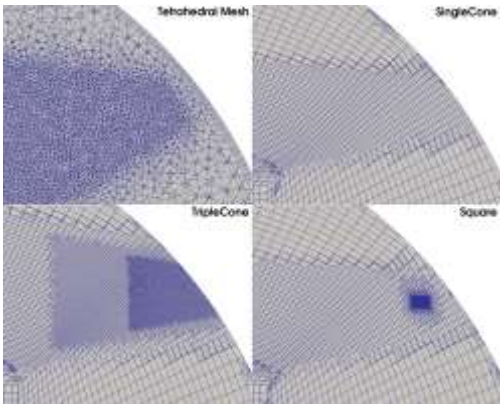

Figure 8: The meshes and their different refinements.

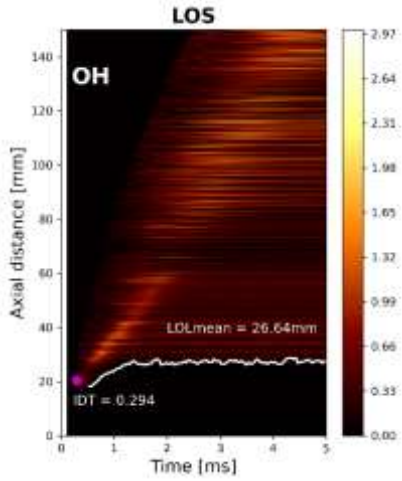

Figure 9: LOS-plot coloured by OH for the Single-Nozzle configuration.

	RANS	EXP
IDT [ms]	0.29	0.48
LOL [mm]	26.5	18
IL [mm]	22±3	20.5

Table 5: Results Single-Nozzle Configuration

In Fig.6 the schematical set-up of the SCC shows the cylindrical shape, featuring a pre-chamber called Regenerator, where air/nitrogen is heated to reach the desired initial conditions before accessing the main chamber. The Regenerator and the main cylindrical chamber are isolated by a non-return valve, thus the CFD domain only consists of the main cylindrical chamber, as shown in Fig.7. In Fig. 8, the refinements around the spray path are

pictured. After a mesh study, the refinement called TripleCone has been chosen for its trade-off between accuracy and computational requirements. The resulting mesh features a minimum cell size of ~420 µm and 1.2Mio cells. This set-up is employed to evaluate reacting simulations (initial conditions in Table 4).

[Test Case] First, the reacting performance have been tested for the Test Case, given the experimental literature available. IDT, LOL and IL have been calculated using an updated version of the I_{xt}-plots approach, the LOS-plot, as explained in [13]. The numerical IDT is shorter (~0.3ms) than the value reported in the reference (~0.48ms). This is expected, as a similar trend was found also for the ECN sprays. The difference though is higher than expected. This may be due to the difference between the fuel used in simulations (n-Dodecane) and experiments (diesel). N-dodecane has a higher cetane number than regular diesel [20]. For the LOL, the mean numerical value is found to be slightly overpredicted (~26mm) compared to the experimental value(~20mm). The Ignition Location (IL) is perfectly in the range (~20mm) of the experimental value (between 18mm and 25mm).

[Nozzle Sizes] Then, since the idea is to relate the combustion parameters of the marine-type nozzles to the ones of Spray D, the ambient conditions in the model are initialized using the same conditions as the ECN benchmark: 15% O_2 concentration instead of 23%, no swirl motion in chamber, 900K and 60 bar. Then, simulations for all the nozzle listed above are carried out and the combustion parameters (IDTs, LOLs and ILs) have been scaled with Spray D's respective values and plotted against the nozzle size in Fig.10, 11 and 12.

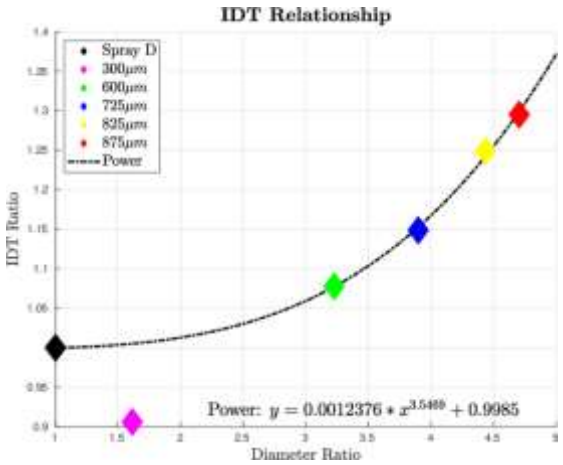

Figure 10: IDT correlation

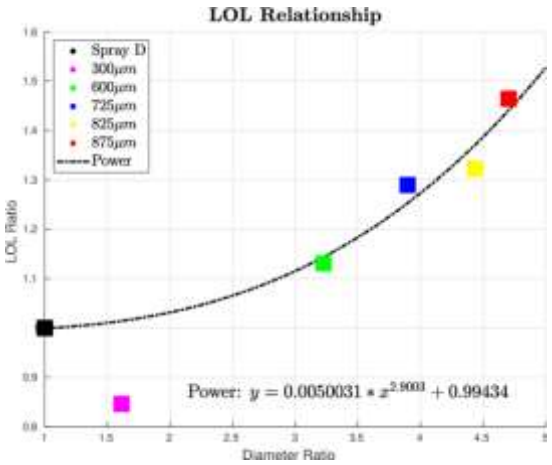

Figure 11: LOL correlation

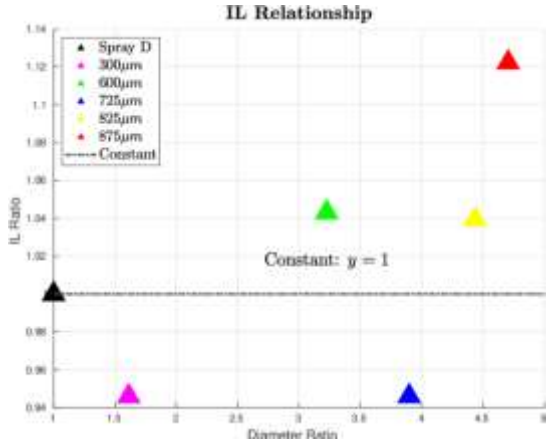

Figure 12: IL correlation

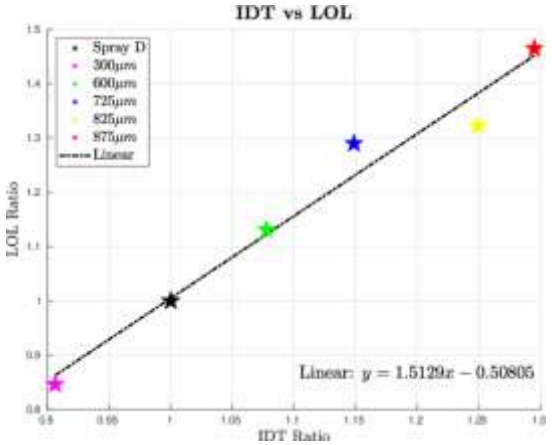

Figure 13: IDT vs LOL relationship

In all graphs, Spray D is colored in black. The dashed line represents the mathematical fit which is also reported in the plots. For IDT the dependency is well captured by a quadratic relation as function of nozzle D. Note that the 300µm is an outlier for which no explanation yet has been found. The LOL also follows a quadratic dependency on the nozzle diameter. A similar trend is also found in [14], but there after 600µm it decreases. Moreover, also for the LOL the 300µm nozzle is an outlier.

To further understand how the IDT and LOL relate to each other with growing nozzle size, in Fig. 13 their correlation is shown. As expected from previous graphs, the 300µm nozzle is the outlier, while the other nozzles show a linear relationship between IDT and LOL with growing nozzle diameter. It is interesting to notice that the increase in LOL with the growing size is higher than the increase in IDT. In fact, a change in the LOL because of diameter variation will change the amount of air entrained (AE) upstream of the LOL which will change the average equivalence ratio downstream. This will affect especially the soot formation. Eventually, it is interesting to notice in Fig. 12 that IL is approximately constant for the different nozzle sizes also for the 300µm , while the largest nozzle slightly deviates from it. The magnitude of the differences in this case, though, are smaller compared to the other parameters. In fact, it is possible to state that the location from the nozzle position of the first ignition is not affected much by the size of the nozzle.

In conclusion, the set of models, already tested for Spray C and D in the previous paragraph, showed good results for the large marine-sized single nozzle from literature, both in inert and reacting conditions. Besides, it was found that both IDT and LOL follow a quadratic dependency with respect to the scaled nozzle diameter. The LOL increases slightly faster than IDT but all correlate nearly linear. Only the 300µm case does not fit well and appears to be an outlier but also follows the linear relation between LOL and IDT. This needs further study. Finally, the IL was found to be hardly dependent on the nozzle diameter. This part of the study is published in [13].

3.1.3 Performance of the SCC model

The final step of the project was the validation in the multi-nozzle configuration of the SCC, for which dedicated experiments have been performed by the project partner WinGD. In fact, these are the first of this kind and no data is available in literature for that matter. Therefore, first the mesh previously validated for the single-nozzle case was checked for the multi-nozzle non-reacting case in terms of liquid length for the conditions of the experimental rig. These are different from the ones of the single-nozzle configuration in Table 4, as shown in Table 6. Then, the reacting simulations were run in the same conditions. The results, in terms of the common combustion parameters, are shown in Fig. 14 and Table 7.

Temperature [K]	**873**
Pressure [bar]	**113**
Swirl [-]	**Yes**
N2 [-]	**0.767**
O2 [-]	**0.233**
CO2 [-]	**0.0**
H2O [-]	**0.0**

Table 6: Initial condition Multi-Nozzle configuration

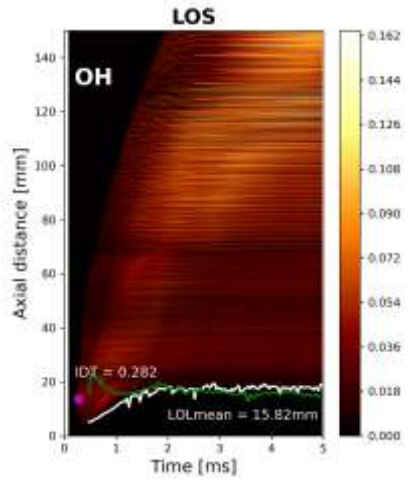

Figure 14: LOS-plot coloured by OH for the Multi-Nozzle configuration. White line: LOL from CFD. Green line: LOL from Exp.

	RANS	EXP
IDT [ms]	0.28	0.44
LOL [mm]	15.82	16.1
IL [mm]	13.5	n.d.

Table 7: Results Multi-Nozzle Configuration

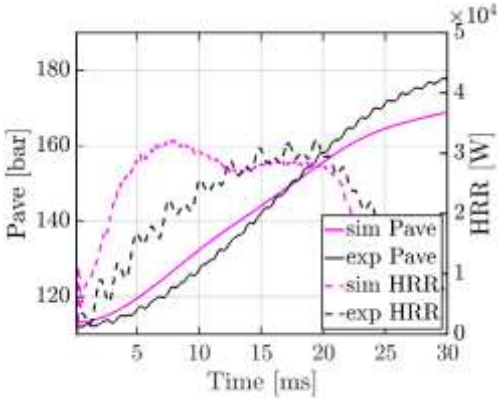

Figure 15: Pave and HRR for Multi-Nozzle configuration

As for the single-nozzle configuration, the IDT is found to be shorter than the experimental data. Though the predicted LOL shows good agreement with the experimental unsteady and mean value, despite the shorter LOL expected for n-Dodecane compared to Diesel. It is worth noting that the time-dependent profile is moving towards the injector at later times. Moreover, the numerical IL, for which an experimental value is not yet available, is upstream compared to the mean LOL, like what was observed in the single-nozzle configuration. Thus, the flame stabilizes farther from the injector than the first ignition kernel.

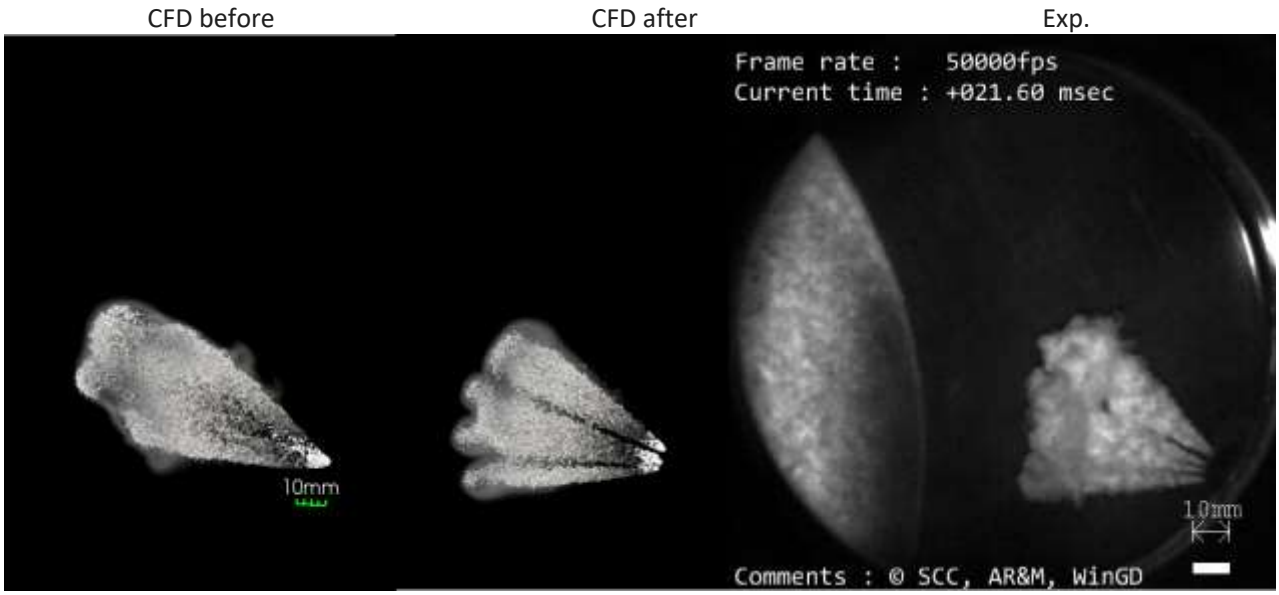

Figure 15: Improvement of the spray shape, visualization of droplets and mixture fraction distribution for CFD

Since the numerical results required improvement, multiple iterations of data exchange with WinGD led the authors to investigate additional parameters, such as average pressure in the chamber (Pave) and heat release rate (HRR), to find the origin of the different behavior. In fact, as depicted in Fig.15, the numerical results show room for improvement, particularly in the first part of the HRR which attests to the early ignition. Therefore, first a study on the injection locations and direction of the sprays in the domain was performed. This led to improved prediction of the droplet and mixture-fraction distribution. Now they closely resemble the experimental

observation (see Fig.16). It proves once more that a close collaboration between experimentalist and numericist is needed to make sure that all relevant parameters are available and correctly implemented in the CFD models. This updated configuration, together with modifications of the table used for the combustion model, strongly improved the IDT, the Pave and the HRR (see Fig.17 and 18 and Table 8).

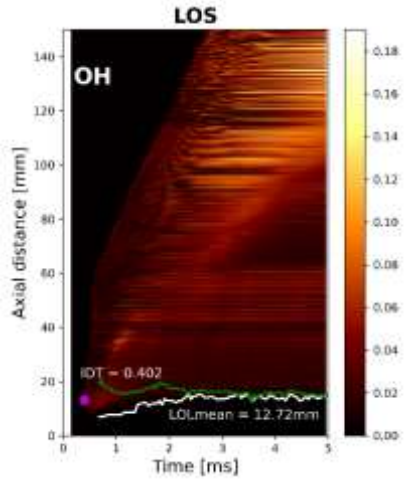

Figure 17: Improved LOS-plot colored by OH for the single-nozzle configuration. White line: LOL from CFD. Green line: LOL from Exp.

	RANS	EXP
IDT [ms]	0.4	0.44
LOL [mm]	12.7	16.1
IL [mm]	13	n.d.

Table 8: Improved Results Multi-Nozzle Configuration

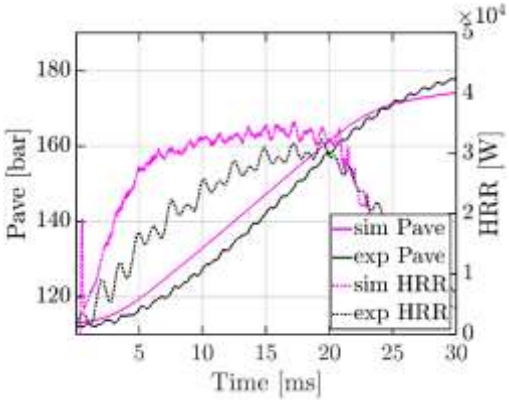

Figure 18: Improved Pave and HRR for multi-nozzle configuration

It is to be noted that the Pave almost perfectly reproduces the experimental trace. The HRR is still not perfect in the range 5 to 10ms but does not show a peak in the same range as it used to happen. This is also reflected by the ID, which is now very close to the experimental value.

Consequently, the set of models prepared in the previous sections performs very well also in a multi-nozzle configuration and is ready for the future switch to renewable fuel. The results of this section are published currently in review process [22].

4 Conclusions and Discussions

4.1 Conclusions

A large and important step has been taken in modelling combustion in large marine-size engines. The only missing step is applying the approach in an engine model. Due to the lack of validation experiments this was not pursued but would have been within reach.

The following steps and main conclusions can be drawn, which follow the routes described above:

- The performance of a computationally expensive (LES) and less-expensive (RANS) turbulence model have been assessed and compared for two ECN Sprays, C and D, using a computational efficient tabulated combustion model, namely Flamelet Generated Manifold (FGM) that allows the use of detailed kinetics. The main conclusion of this work is that the efficient RANS turbulence model coupled with the FGM combustion model provides comparable results to the more detailed and computationally expensive LES.
- Given the large difference in size between the nozzles used as benchmark and the ones in the SCC, a study on the influence of the nozzle diameter on the combustion properties has been carried out. It was found that the Ignition Delay Time and Lift-Off Length follow a quadratic dependency with respect to the nozzle diameter, while the Ignition Location is hardly dependent on it.
- Eventually, the same settings and model have been used for the SCC in single- and multi-nozzle configuration. Although a similar effort was present for single nozzle layout in literature, for the multi-nozzle design this was a first time as far as the authors know. Therefore, a careful comparison of the numerical outcome with the experimental data, led to promising results in terms of the main combustion parameters.

In conclusion, the combination of the RANS turbulence model and the FGM combustion model has proven to be very efficient and reliable. The work shows that the approach FGM in a RANS setting can be used to determine the impact of fuel chemistry in large two-stroke marine engines. As such it gives great confidence it can assess the impact of a blending a bio-HFO in a reference marine fuel on the performance of such engines if adequate chemical models exist for these types of fuels which was the main goal of the project.

4.2 Deviations from the DoA

- Modelling 4-stroke engines was not pursued as it became clear that even litre scale relevant Bio-HFO and their blends were not becoming available. Experimental data is of utmost importance to set up a reliable CFD model.
- Modelling 2-stroke large engines for the same reason were not pursued.

Instead, much emphasis was put on developing adequate models and validating them on detailed data from the Spray Combustion Chamber (SCC, see deliverable 4.2).

5 References

[1] J. E. Dec, A conceptual model of DI diesel combustion based on laser-sheet imaging*, p. 970873. doi:10.4271/970873.
[2] A. Krisman, E. R. Hawkes, M. Talei, A. Bhagatwala, J. H. Chen,Characterisation of two-stage ignition in diesel engine-relevant thermochemical conditions using direct numerical simulation doi: 10.1016/j.combustflame.2016.06.010.
[3] R. N. Dahms, G. A. Paczko, S. A. Skeen, L. M. Pickett, Understanding the ignition mechanism of high-pressure spray flames 36 (2) 2615–2623.doi:10.1016/j.proci.2016.08.023.
[4] E. C. Network, https://ecn.sandia.gov/ (2023).
[5] N. Maes, M. Meijer, N. Dam, B. Somers, H. Baya Toda, G. Bruneaux, S. A. Skeen, L. M. Pickett, J. Manin, Characterization of Spray A flame structure for parametric variations in ECN constant-volume vessels using chemiluminescence and laser-induced fluorescence, Combustion and Flame 174 (2016) 138–151. doi:10.1016/j.combustflame.2016.09.005.
[6] J. Garcıa-Oliver, R. Novella, J. Pastor, L. Pachano, Computational study of ECN spray a and spray d combustion at different ambient temperature conditions 2 100027. doi:10.1016/j.treng.2020.100027.
[7] A. Di Matteo, H. Bao, B. Somers, Modeling spray c and spray d with FGM within the framework of RANS and LES, Frontiers in Mechanical Engineering 8 (2022) 1013138. doi:10.3389/fmech.2022.1013138.
[8] K. Herrmann, Reference data generation of spray characteristics in relation to large 2-stroke marine diesel engines using a novel spray combustion chamber concept, 23rd Annual Conference on Liquid Atomization and Spray Systems (2010).
[9] B. von Rotz, H. K., Impact of evaporation, swirl and fuel quality on the characteristics of sprays typical of large 2-stroke marine diesel engine combustion systems (2011).
[10] K. Herrmann, B. Schneider, K. Boulouchos, A ”Spray Combustion Chamber” facility for investigations in relation to large 2-stroke marine diesel engine combustion system optimization, Proceedings of the International Symposium on Marine Engineering (2011).
[11] A. Schmid, K. Boulouchos, Ignition behavior of marine diesel sprays investigation of marine diesel ignition and combustion at engine-like conditions by means of OH* chemiluminescence and soot incandescence, The Eighth International Conference on Modeling and Diagnostics for Advanced Engine Systems (2012).
[12] M. Bolla, M. A. Cattin, Y. M. Wright, K. Boulouchos, R. Schulz, 3D-CFD lagrangian spray simulations for large two stroke marine diesel engines compared with experimental data of a spray combustion chamber, in: ASME 2012 Internal Combustion Engine Division Spring Technical Conference, American Society of Mechanical Engineers, 2012, pp. 1–9. doi:10.1115/ICES2012-81016.
[13] A. Di Matteo, B. Somers, ”A study on the relationship between ECN spray D and Marine-Sized nozzles using FGM combustion model”, https://doi.org/10.4271/2024-01-2695
[14] M. Bolla, A. Srna, Y. M. Wright, B. Von Rotz, K. Herrmann, K. Boulouchos, Influence of injector diameter (0.2-1.2 mm range) on diesel spray combustion: Measurements and CFD simulations, SAE Technical Papers (2014). doi:10.4271/2014-01-1419.
[15] OpenFOAM, https://openfoam.org/version/7/ (2023).
[16] J. V. Oijen, Flamelet-generated manifolds: development and application to premixed laminar flames, Ph.D. thesis, Technische Universiteit Eindhoven (2002).
[17] N. Peters, Laminar diffusion flamelet models in non-premixed turbulent combustion, Progress in Energy and Combustion Science 10 (3) (1984)632 319–339. doi:10.1016/0360-1285(84)90114-X.
[18] T. Yao, Y. Pei, B.-J. Zhong, S. Som, T. Lu, K. H. Luo, A compact skeletal mechanism for n-dodecane with optimized semi-global low temperature chemistry for diesel engine simulations, Fuel 191 (2017) 339–349. doi:10.1016/j.fuel.2016.11.083
[19] Payri, F., García-Oliver, J.M., Novella, R., Pérez-Sánchez, E.J., 2019. Influence of the n-dodecane chemical mechanism on the CFD modelling of the diesel-like ECN Spray A flame structure at different ambient conditions. Combustion and Flame 208, 198–218. https://doi.org/10.1016/j.combustflame.2019.06.032
[20] R. Payri, F. Salvador, J. Gimeno, and J. E. Peraza, “Experimental study of the injection conditions influence over n-dodecane and diesel sprays with two ECN single-hole nozzles. Part II: Reactive atmosphere,” Energy Conversion and Management, vol. 126, pp. 1157–1167, Oct. 2016.
[21] H. B. Siebers D.L., “Effects of injector conditions on the flame lift-offlength of di diesel sprays,”
[22] A. Di Matteo, B. Somers, “FGM Combustion Model Performance in a Simplified Naval Engine Combustion

Chamber", Currently under review in FUEL, (2024).
[23] Large Eddy Simulation of Diesel Spray Combustion with Flamelet Generated Manifolds. / Akargün, Hayri Yigit. Eindhoven: Eindhoven University of Technology, 2021. 119 p., https://research.tue.nl/files/183284207/20210915_CO_Akargun_hf.pdf
[24] R.D. Reitz, "Modeling Atomization Processes in High-Pressure Vaporizing Sprays.", 1987

6 Acknowledgement

The author(s) would like to thank the partners in the project for their valuable comments on previous drafts and for performing the review.

Project partners:

#	Partner short name	Partner Full Name
1	TUE	Technische Universiteit Eindhoven
2	VERT	Vertoro BV
3	T4F	Tec4Fuels
4	BLOOM	Bloom Biorenewables Ltd
5	UNR	Uniresearch B.V.
6	WinGD	Winterthur Gas & Diesel AG
7		(Formerly SeaNRG, is now GOODFUELS #12)
8	TKMS	Thyssenkrupp Marine Systems GMBH
9	OWI	OWI – Science for Fuels gGmbH
10	CSIC	Agencia Estatal Consejo Superior De Investigaciones Cientificas
11	VARO	Varo Energy Netherlands BV
12	GOOD	GoodFuels B.V.

This project has received funding from the European Union's Horizon 2020 research and innovation programme under grant agreement No 883753